Development of New High Temperature Plasma Sources for Spectrochemical Analysis: Multivariate Optimization by the Modified Sequential Simplex Method

Gae Ho Lee

Department of Chemistry, Chungnam National University, Taejon 305-764
Received October 30, 1992

The new high temperature plasma source for spectrochemical analysis has been developed and characterized. In the development of new high temperature plasma sources for atomic emission spectrocopy, optimization of experimental variables is necessary to achieve the best analytical results. By means of a modified sequential simplex optimization method, six experimental variables were optimized. The line-to-background (L/B) ratio for Ca(II) at 393.37 nm was used as measure of the response function. The optimal experimental conditions were found to be at a current of 27.8 A, a plasma length of 28.8 mm, a sample uptake rate of 1.3 ml/min, a sample carrier gas flow rate of 0.7 ml/min, a plasma gas flow rate of 4.9 *l*/min, and an observation height of 6.4 mm above the top quartz tube.

Introduction

The atomic spectroscopy has long been used for the analysis of trace elements and certain nonmetals such as boron and phosphorus[1-5]. Especially, investigation and characterization of atomization source used in atomic emission spectroscopy is important since the stability and reproducibility of analytical results are greatly affected by the performance of atomization source. Atomic emission spectroscopy is a process whereby the light emitted by excited atoms and ions is measured. After excitation of a free atom or ion to an unstable energy state by sufficient collisional energy, emission occurs when the excited atom or ion returns to a lower state or the ground state. The wavelengths of radiation emitted are specific to the elements present in the sample to be analyzed. Due to the nature of atomic emission spectroscopy, the excitation source is a very critical component in atomic emission instruments. Electrical discharges sources such as DC and AC arcs, high voltage spark source, and flame have long been used as atomization sources in atomic emission spectroscopy. Recently, the developments of the ICP[6,7] and DCP[8,9] have caused a dramatic increase in utilizations of the atomic emission spectroscopy and a virtual renaissance of atomic emission spectroscopy in handling solutions, because they do not exhibit many of the problems associated with past excitation sources.

However, the major shortcoming for most electrical plasma sources, especially in the case of 3-electrode commercial DCP, is their inability to obtain sufficient contact between the hot plasma and the sample aerosol stream. In addition, since sample must pass the discharge region of the 3-electrode DCP, the power dissipation will be varied from sample to sample. As a result, the excitaiton and ionization mechanisms of 3-elctrode DCP are more complicate than those of ICP.

In general, both the initial and operating costs for plasma emission techniques, especially for the ICP source, are relatively expensive. The operating costs for an ICP are mainly due to gaseous of liquid argon for the nebulizer and gas flows (usually 12 to 20 *l*/min) to the torch. Thus many scientists, including the commercial ICP manufactures, have conducted extensive researches for several years in order to modify standard ICP torch design to reduce the radio-frequency power and the argon gas-flow requirements without sacrificing the analytical performance of the standard ICP torch.

In the previous experiment[10-12], high temperature plasma source has been developed and characterized. In this way, the problems described above can be overcome by the use of electrodes for helping to control the shape of the plasma, which allows the efficient entrainment of an aerosol sample stream in the center of hot plasma over longer periods of time. Although spectral interference from the atoms in the electrode material occasionally occur, the observation regions of the new high temperature plasma sources are not located in current-carrying columns, so that high plasma background continuum emission is elminated in the measurement of analytical signals.

However, the optimization of the experimental variables is important for the new plasma sources to ensure the best analytical performances. Several systematic experimental methods are available for the optimization. The factorial experimental method[13,14] is most powerful when used to detect differences caused by two or more discrete possibilities. This method is often used to evaluate the relative singificance of several experimental variables. The factorial design can explore either a small region comprehensively or a large region superficially. Therefore, a very large number of experiments would often be required to determine an optimum condition precisely. The one-factor-at-a-time method[14,15] is probably one of the most common techniques of optimization in analytical chemistry when the experimental variables can be changed quickly and continuously over wide range. If the experimental variables do not interact with each other, each experimental variable could be optimized independently of the other experimental variables. However, since the experimental variables in the new high temperature plasma source are closely interrelated with each other (this is also true for an inductively coupled plasma, ICP), a traditional one-factor-at-a-time investigation may be potentially misleading. The simplex optimization has proven to be a simple, fast, and effective means of optimizing system which have

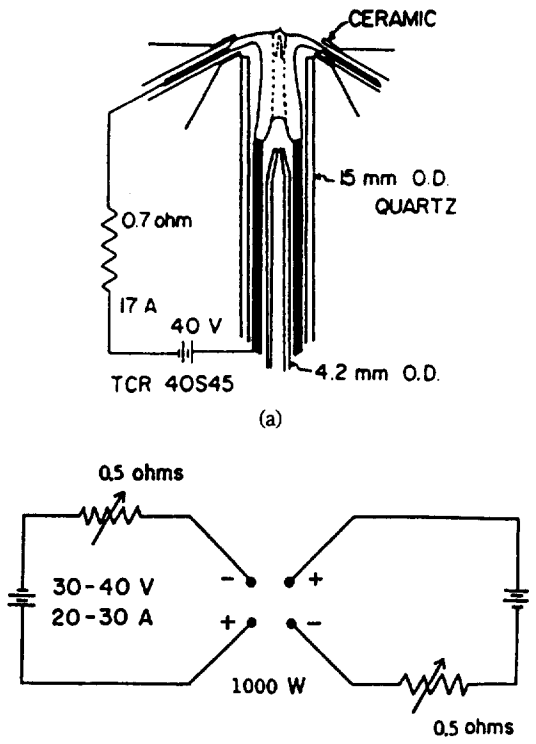

Figure 1. Schematic Diagram of New High Temperature Plasma Sources for Atomic Emission Spectrometer. a) The plasma source for emission, b) Electrical circuit.

interrelated experimental varioables. As a result, the modified sequential simplex optimization method[16-19], which allows numerous interrelated experimental variables to be optimized, was employed in order to search for the optimum experimental conditions in this study. A one-factor-at-a-time experiment[10-12], in which five of the experimental variables were held constant and the sixth varied as the L/B ratio was measured, was used to confirm the success of the simplex optimization.

Experimental

The experimental facilities for the new high temperature plasma source used in this study are similar to those described proviously[10-12]. The schematic diagram of new high temperature plasma source is shown in Figure 1a. The electrical circuit used for the formation of the plasma is shown in Figure 1b.

In this experiment, the investigation of the plasma source for emission has been performed for the first time. The most critical component of the entire new plasma source is the plasma tube arrangement and its design. The outer and inner diameter of the concentric quartz tubes were examined and the dimensions of the three concentric precision quartz tube were found to be critical. The following factors have been considered to obtain the optimum diameters of the concentric quartz tubes.

Due to a combination of high temperature and pressure of the plasma discharge, sample aerosols introduced into the plasma discharge tend to flow around the high temperature regions of the discharge. Also with low velocity of the sample carrier gas, the sample aerosol stream tends to spread out from a tip of a sample introduction tube instead of remaining constant in width. Consequently, the inner diameter of the tip of the sample introduction tube has to be small enough to generate a relatively high velocity of smaple aerosol stream in order to pass through the plasma. In addition, a small inner diameter of the tip of the sample introduction tube is also needed to produce a small sample aerosol stream that can be effectively surrounded by the plasma columns for better desolvation, atomization, and excitation of analyte species.

An inner diameter of 1.0 mm to 1.5 mm was found to be the best for the new plasma sources with Meinhard concentric nebulizer. Since about 0.7-1.0 *l*/min of sample aerosel carrier gas flow rate is required to generate fine aerosols with the Meinhard concentric nebulizer, the above sizes of sample tips are suitable to provide the small sample aerosol stream required for effective contact with the plasma columns and a relatively long residence time. In addition, the inner diameter of the sample introduction tube has to be large enough to avoid back pressure and the condensation of sample aerosol on the wall of the inside of the sample introduction tube.

The inner diameter of the inner quartz tube is chosen initially, taking into account both the amount of argon gas consumed per unit time and the length of the plasma column. The larger the inner diameter of the inner quartz tube is the more argon gas was required to sustain a stable discharge. If a large inner diameter is chosen, then this is the factor that will mainly limit the minimum consumption of the argon gas. On the other hand. the inner diameter has to be large enough so that the gap between the plasma columns is wide enough to pass the sample aerosol through the plasma columns without extinguishing them. As in a conventional ICP torch, an inner quartz tube with a 12.6 mm inner diameter and 1 mm wall thickness was selected for our application.

In our application, the stabilization gas is used to push the parallel plasma columns and the sample. In the ICP, the stabilizing gas is used to prevent the quartz tubes walls from melting and to position the plasma discharge radially at the center of the tube. More importantly, the stabilizing gas is used to help from the discharge into an annular shape through which a sample aerosol can be transported by the sample aerosol carrier gas. In the ICP, a vortex stabilization is accomplished by introducing a gas into a plasma tube tangentially, which causes it to flow spirally down the walls. Therefore, the tangential flow of the argon gas, which is typically in the 10 *l*/min range, for a conventional ICP torch is very critical for the analytical performance of the ICP, as is also the annular spacing between the outer and inner quartz tubes. The vortex stabilization flow with high velocity was obtained with 0.20 mm annular spacing between the inner and outer quartz tubes. With the commercial precision bore quartz tubing, a 15.00 mm inner diameter outer quartz tube was selected for the our application in order to get on annular spacing of 0.20 mm between the inner and outer

Table 1. Possible Experimetal Variables and Response Functions in the New High Temperature Plasma Source

Experimental Variables
Current
Length of Plasma
Observation Height
Sample Carrier Gas Flow Rate
Plasma Gas Flow Rate
Sample Uptake Rate
Position of tip of the Sample Introduction Tube
Sizes of Quartz tubes
Diameter of Electrodes
Response Functions
Line/Background Ratio
Signal/Noise Ratio
Precision
Atom/Ion Line Intensity
Emission Intensity
Excitation Temperature
Electron Number Density

quartz tubes.

Results and Discussion

In the new plasma source, the possible experimental variables and response functions are listed in Table 1. Preliminary experiments showed that several experimental variables which affected the analytical performance of the plasma source were closely interrelated with each other. For example, as the sample carrier gas flow rate is increased, the point for the maximum emission intensity shifts to a higher position in the discharge. Consequently, the optimal sample carrier gas flow rate will be different from region to region in the plasma. In additions, the position of the point for the maximum emission intensity significantly affected by varying the current and the length of plasma. Thus a true optimum experimental condition cannot be readily achieved by varying one factor while keeping the others constant.

In order to perform the modified sequential simplex optimization[16-19] for the plasma source successfully, the experimental variables had to be chosen very carefully. Among the possible experimental variables in the plasma, the six chosen variables, such as current, length of plasma, observation height, flow rate of the sample carrier gas, flow rate of the plasma gas, and sample uptake rate, were selected to be optimized based upon the following considerations. First, because of the nature of the operation of the modified sequential simplex optimization, each experimental variable should be readily adjustable by the operator during the operation of the plasma without the interruption. Since the sizes of the quartz tube and electrodes were impossible to change without extinguishing the plasma during operation, those variables were eliminated from the modified sequential simplex optimization. Second, in the selection of experimental variables for simplex optimization, all experimental variables which are thought to have a possible effect on the response should be included. However, the investigation of the position of tip for the sample introduction tube which is considered to be insignificant was omitted in this study. For the plasma source used in this study, the significance of each experimental variable has already been determined in a previous one-factor-at-a-time experiment[10-12].

Table 2. Boundaries for the Experimental Variables to be Optimized

Variables	Lower bound	Upper bound
Current, A	20.0	30.0
Length of Plasma, mm	10.0	40.0
Observation Height, mm*	0.0	10.0
Sample Carrier Gas, /min	0.5	1.0
Plasma Gas, *l*/min	2.0	5.0
Sample Uptake Rate, m*l*/min	0.3	1.3

*Observation height is expressed by the distance above the top of the quartz tube.

The possible reponse functions optimized in this study are also listed in Table 1. In this single-element optimization study, due to simplicity, the line-to-background (L/B) ratio for the Ca(II) at 393.37 nm was selected as a response function. The lower and upper bounds for the six experimental variables to be optimized are listed in Table 2. The boundary for each experimental variable is defined by various practical considerations, especially by the physical limits of the instruments since the simplex may well require experimental conditions beyond the capabilities of the instruments.

The variable step-size simplex optimization algorithm in this study was basically the same as that suggested by Nelder and Mead[16-19] was used. With the continuous introduction of 10 mg/*l* of Ca standard solution into the plasma, the L/B ratio of the Ca(II) at 393.37 nm was optimized. The L/B ratio at each vertex was determined from the mean value of 32 measurements each with 1-s integration time in order to reduce the effect of noise on the simplex optimization.

At the beginning of the simplex, a relatively large initial step size was chosen to ensure that most of the factor space was explored before the simplex collapses onto the optimum. When the simplex indicates the instrumental settings beyond the physical limits of the instruments, the simplex is forced back into bounds. However, boundary violations did not occur during our experiment, except for the sample uptake rate at the end of the simplex operation. Finally, the simplex was stopped when the step size became less than 2% of the domain of each experimental variables.

The result of the simplex optimization for the new plasma source is shown in Figure 2, illustration the variations in L/B ratios as a function of simplex vertex number. The vertices for the failed movements are also included in this figure. The trend in Figure 1 demonstrates the rapid improvement in L/B ratio during the course of the simplex optimization. Compared with the L/B ratios at the beginning of the simplex optimization, the progress towards the optimum by the simplex procedure was fairly rapid in this study. The simplex optimization was halted at the 56th vertex and the L/B ratio was found to be 207. However, it should be pointed out that the best L/B ratio was obtained at the 36th vertex.

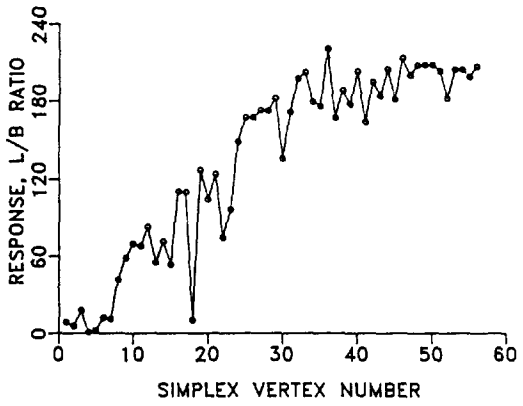

Figure 2. Movement of the L/B ratio as a function of the simplex vertex number (The L/B ratio for the Ca(II) at 393.37 nm was used as a response function in this study).

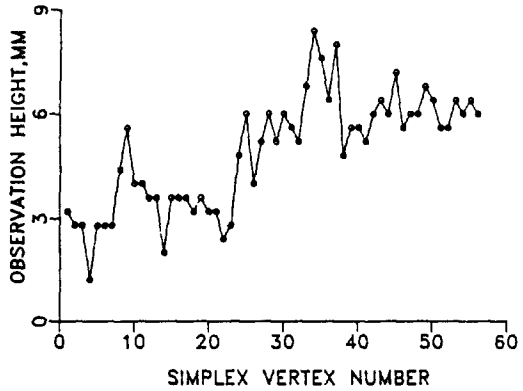

Figure 3. Movement of the observation height as a function of the simplex vertex number. The observation height is expressed by the distance above the quartz tube.

Since this was due to a brief moment of excessive signal associated with burning of an impurity in the electrode, the L/B ratio at the 36th vertex was not considered to be an optimum.

Figure 3 illusrates that there is a trend, during the optimization, for the optimal observation height to shift higher in the plasma. The optimal observation height was determined to be 6.4 mm above othe quartz tube, which is in good agreement with the results of a previous one-factor-at-a-time experiment[10-12]. It also showed that the optimal observation height in the new high temperature plasma source was 6 to 8 mm above the quartz tube, as shown in Figure 4, demonstrating the vertical net emission intensity profile for the Mg ion line. The optimal observation points for both the neutral atom and ion lines occurs between 6 and 8 mm above the quartz tube. However, it indicates that the optimal observation point is not grealy changed by varying the current for the 25 mm plasma length. Figure 5 shows that the response surface of the observation height as a function of the vertex number.

Figures 6 and 7 show the plot and the response surface of the length of the plasma as a function of the simplex vertex number. The optimal length of the plasma was found to be 28.8 mm. There was not much change in the length

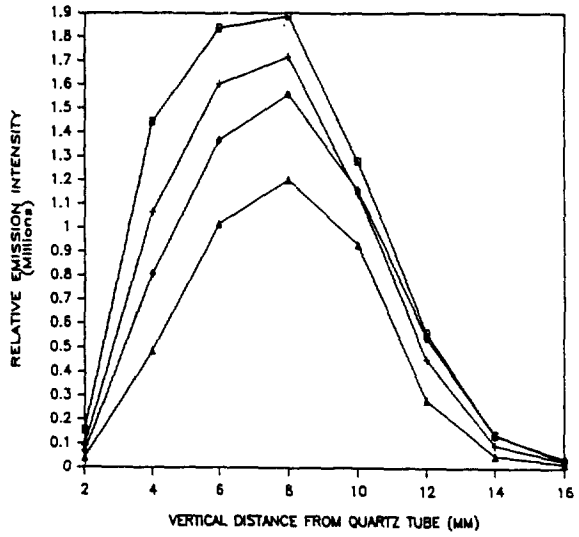

Figure 4. Vertical distribution of the 280.27 nm Mg ion line emission intensity at the center of the plasma for 4 currents. (□) 19 A; (+) 18 A; (◇) 17 A; (△) 16 A. The length of the plasma is 25 mm.

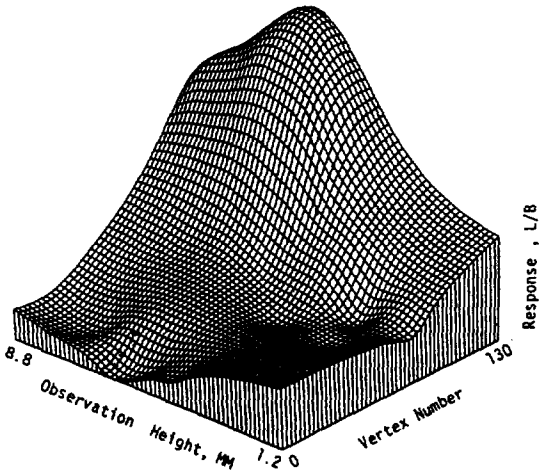

Figure 5. Response Surface of the Observation Height as a function of the simplex vertex number.

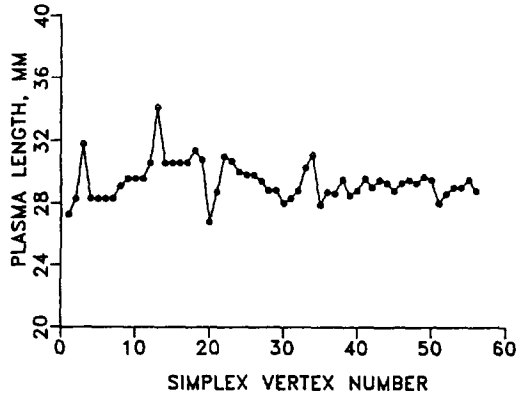

Figure 6. Movement of the length of plasma as a function of the simplex vertex number.

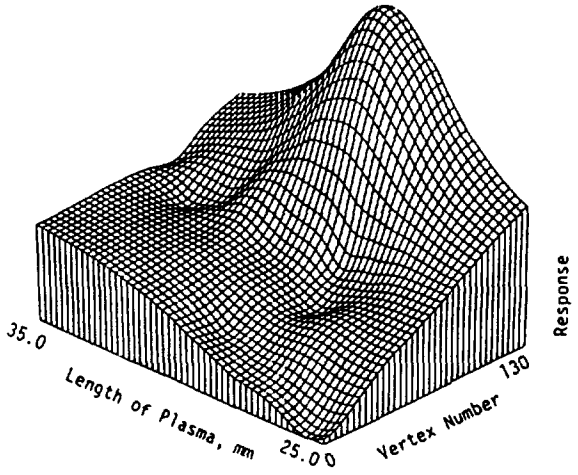

Figure 7. Response Surface of the length of plasma as a function of the simplex vertex number

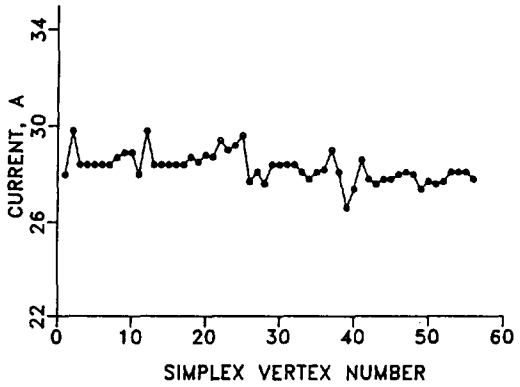

Figure 8. Movement of the current as a function of the simplex vertex number.

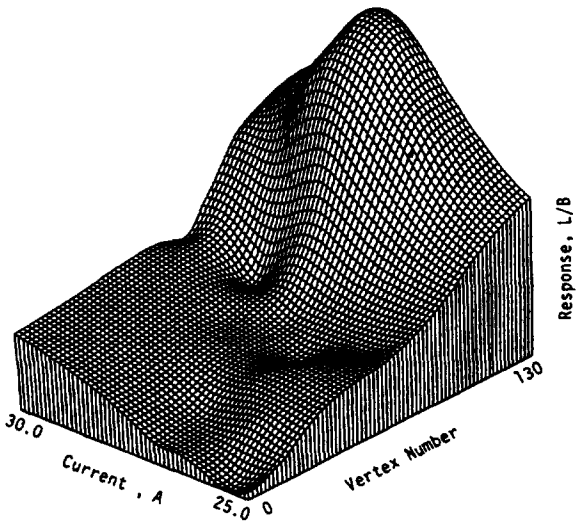

Figure 9. Response surface of the current as a function of the simplex vertex number.

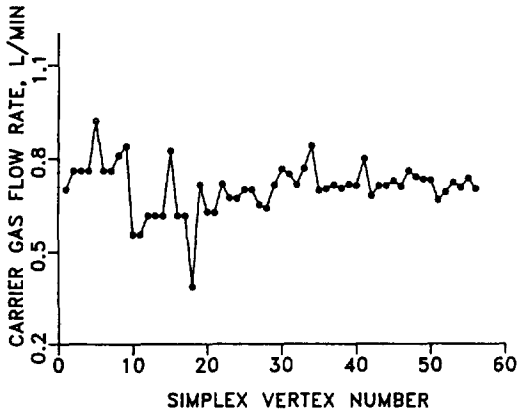

Figure 10. Movement of the sample carrier gas flow rate as a function of the simplex vertex number.

of the plasma during the optimization, indicating the initial plasma length (27 mm) was long enough to desolvate, vaporize, atomize, and excite the analyte species. For the plasma source used in this study, the length of plasma is one of the most important experimental parameters. One of the main advantages of this plasma source is that the length of the plasma can be readily controlled by moving the lower electrodes up and down even during the operation. Consequently, the residence time experienced by the analyte species can be adjusted to provide sufficient time to atomize and excite an aerosol sample. Thus, analytical performance is singificantly affected by varying the length of plasma. In this way, high solid content sample can be easily analyzed without difficulties occurred in the conventional plasma sources such as ICP and DCP.

Moreover, narrower horizontal net emission intensity profiles for the shorter lengths of the plasma are observed. As the length of plasma is shortened, the sample aerosol stream becomes physically wider because of the reduced confining effect of the shorter plasma columns. Even though the widths of the sample aerosol stream for the shorter plasma lengths are wider than those for the long plasmas, analyte species have less time to diffuse horizontally away from the sample stream, causing narrower horizontal emission intensity profile. This is probably due to the reduced energy transfer between the plasma and sample, resulting in less atomization and ionization.

A plot of a current as a function of the simplex vertex number and response surface are shown in Figures 8 and 9, respectively. The optimal current for the plasma was found to be 27.8 A. As the current was increased, the L/B ratio decreased due to the higher plasma background emission. In addition, the shift of the point of the maximum intensity to the lower position in the plasma was observed, resulting in a decrease in L/B ratio. The horizontal emission profiles for the lower current are observed to be narrower. Since the plasma column radius is increased by increasing the current, improved contact with the sample aerosol for the higher current plasma results in more effective heat transfer from the plasma to the sample aerosel.

According to the model developed by Boumans[20] for a free-burning arc in air, the power dissipated per centimeter in the arc column is proportional to the square of the current and is inversely proportional to the electrical conductivity of the gas. And the electrical conductivity of the gas is pro-

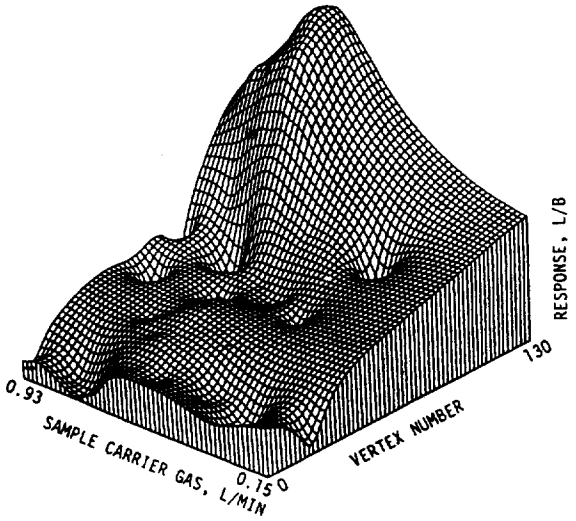

Figure 11. Response surface of the sample carrier gas flow rate as a function of the simplex vertex number.

portional to the square of the column radius. Therefore, if the plasma column radius, hence its electrical conductivity, is increased by increasing the current, the power dissipation per unit length in the arc column would not be substantially changed. Thus the temperature in the arc column in rather insensitive to the arc current. As a result, rather than the temperature of the arc column, the efficiency of the heat transfer to the sample aerosol in the plasma source caused by the change in plasma shape may be the main factor causing different horizontal emission profiles at different current levels.

Figure 10 and 11 illustrate the movement of the sample carrier gas flow rate and response surface asa function of the simplex vertex number, respectively. The result demonstrates that a flow rate of 0.7 *l*/min for the sample carrier gas is optimum for the plasma. This was confirmed by the previous one-factor-at-a-time experiment, which showed that flow rate of 0.7 *l*/min for the sample carrier gas provided not only sufficient residence time for the analyte species in the plasma, but effective nebulization of sample with the Meinhard concentric nebulizer.

The sample carrier gas flow rate is one of the most important experimental factor in this study. Since the two parallel plasma columns are oriented perpendicular to the direction of the upward sample aerosol stream, the fast flow rate of the sample carrier gas caused plasma fluctuations, resulting in noise and drift in the analytical signals and even the eventual extinction of the plasma. Although the lower gas flow rate stabilizes the plasma and assures longer residence time of the analyte species and better contact with the plasma columns, it is not feasible to make fine sample aerosols using Meinhard concentric nebulizer with such a low flow rate. Therefore, significant volatilization interferences are observed because of the large aerosol droplets produced by the lower flow rates (less than 0.5 *l*/min). Comparing to the previous response surface for the length of plasma, current, and observation height, the response surface for the sample carrier gas flow rate shows more roughness.

Figure 12 shows the variations of the plasma gas flow

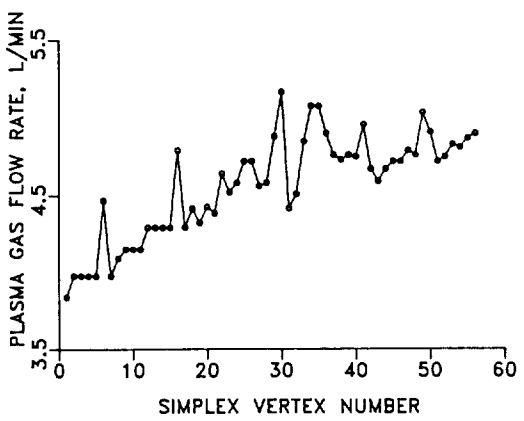

Figure 12. Movement of the plasma gas flow rate as a function of the simplex vertex number.

rate as a function of the simplex vertex number. There was gradual increase in the sample uptake rate during the simplex optimization. Optimal experimental conditions were found to be at a sample uptake rate of 1.3 ml/min, a value which is about one-half of the free uptake rate. And the optimal condition of the plasma gas flow rate is found to be 4.9 *l*/min. As the simplex moves toward the optimum, there is a trend for the background emission intensity to decreases gradually.

In conclusion, the performance of modified sequential simplex optimization was rapid and successful in this study. The optimum experimental conditions were achieved in approximately 45 steps and agreed with one-factor-at-a-time searches in a previous study. Although the simplex method did not provide complete information on the influence of each experimental variable on the performance of the plasma, the optimum experimental conditions for the plasma source were obtained relatively fast and easily.

Acknowledgement. This work was supported by a research grant (903-0304-017-2) from the Korea Science and Engineering Foundation.

References

1. D. W. Golightly and J. L. Harris, *Appl. Spectrosc.*, **29**, 233 (1975).
2. C. D. Keirs and T. J. Vickers, *Appl. Spectrosc.*, **31**, 273 (1977).
3. S. R. Ellebracht, C. M. Fairless, and S. E. Manahan, *Anal. Chem.*, **50**, 1649 (1978).
4. G. W. Johnson, H. E. Taylor, and R. K. Skogerboe, *Spectrochim. Acta*, **34B**, 197 (1979).
5. R. J. Decker, *Spectrochim. Acta.*, **35B**, 19 (1980).
6. S. Greenfield, I. Ll. Jones, and C. T. Berry, *Analyst*, **89**, 713 (1964).
7. R. H. Wendt and V. A. Fassel, *Anal. Chem.*, **37**, 920 (1965).
8. S. E. Valente and W. G. Schrenk *Appl. Spectrosc.*, **24**, 197 (1970).
9. R. J. Decker, *Spectrochim. Acta*, **35B**, 19 (1980).
10. G. H. Lee, J. P. Shields, and E. H. Piepmeier, *Spectrochim. Acta*, **43B**, 1273 (1988).

11. G. H. Lee, J. P. Shields, and E. H. Piepmeier, *Spectrochim. Acta*, **43B**, 1485 (1988).
12. J. P. Shields, Gae H. Lee, and E. H. Piepmeier, *Appl. Spectrosc.*, **42**, 684 (1988).
13. S. L. Morgan and S. N. Deming, *Anal. Chem.*, **46**, 1170 (1974).
14. L. Ebdon, M. R. Cave, and D. J. Mowthorpe, *Anal. Chem. Acta*, **115**, 179 (1980).
15. S. Greenfield and D. T. Burns, *Anal. Chim. Acta*, **113**, 205 (1980).
16. J. A. Nelder and R. Mead, *Computer J.*, **7**, 308 (1965).
17. S. N. Deming and S. L. Morgan, *Anal. Chem.*, **45**, 278A (1973).
18. L. A. Yarbro and S. N. Deming, *Anal. Chim. Acta*, **73**, 391 (1974).
19. A. E. Brookes, J. J. Leary, and D. W. Golightly, *Anal. Chem.*, **53**, 720 (1981).
20. P. W. J. M. Boumans, Theory of Spectrochemical Excitation, Plenum, New York, U.S.A. (1966).

Catalytic Hydrogenation of Aromatic Nitro Compounds over Borohydride Exchange Resin Supported Pd (BER-Pd) Catalyst

Nung Min Yoon*, Hyang Won Lee, Jaesung Choi and Hyun Ju Lee

Department of Chemistry, Sogang University, Seoul 121-742
Received November 4, 1992

Aromatic nitro compounds are selectively hydrogenated to the corresponding amines in high yields at room temperature and atmospheric pressure using BER-Pd catalyst without affecting ketone, ether, ester, nitrile or chloro groups also present. Especially the nitro group in 4-nitrobenzyl alcohol, methyl 4-nitrobenzyl ether and N-N-dimethyl 4-nitrobenzylamine is selectively hydrogenated with this catalyst to give the corresponding amines without hydrogenolysis of benzylic groups. And aromatic nitro compound can be reduced selectively in the presence of aliphatic nitro compound.

Introduction

Selective catalytic hydrogenation of aromatic nitro groups is important in organic synthesis, particularly when a molecule has several other reducible moieties. Although platinum, palladium or nickel catalysts may be used, nickel catalyst usually requires high pressure and platinum catalyst is regarded more selective than palladium[1] especially when the nitroaromatics also contain benzylic groups[2] or halogen[3]. Sometime ago carbon supported platinum catalyst was produced *in situ* by borohydride reduction, and nitroaromatics could be rapidly reduced to the corresponding amino derivatives at room temperature and atmospheric pressure[4].

On the other hand, Borohydride Exchange Resin (BER), readily prepared from anion exchange resion (chloride form) and aqueous sodium borohydride solution[5], is an quarternary ammonium borohydride, borohydride ion being attached on the resin. It exhibits unique reducing characteristics[6a,b] in alcoholic solvents besides the simple work up procedures[6a]. In this paper we wish to report the preparation of palladium catalyst on BER (BER-Pd) and selectivity of the catalyst in the reduction of nitroaromatics.

Results and Discussion

Preparation of Borohydride Exchange Resin Supported Palladium (BER-Pd). BER (0.5 mmol in BH_4^-) was placed in the reactor flask of Brown automatic hydrogenator[7], and flushed with nitrogen. Solution of $PdCl_2$ (0.05 mmol) in 20 m*l* ethanol (95%) was added with stirring at room temperature. Hydrogen evolution ceased in 10 min, and the preparation of BER-Pd is completed. Hydrolysis of BER-Pd thus prepared revealed the existence of approximately 0.45 mmol of BH_4^-.

Characteristics of BER-Pd Catalyst. We studied briefly the effect of temperature and catalyst/substrates ratio on the reduction of nitrobenzene. When 10 mmol of nitrobenzene is hydrogenated over 0.05 mmol Pd on BER-Pd, the hydrogenation was completed in 220 min at 0℃, 90 min at 25℃ and 80 min at 40℃. Therefore we carried out hydrogenation at room temperature. When we changed the amount of nitrobenzene hydrogenated on the fixed amount of BER-Pd (0.05 mmol) from 5 to 10, 25, 50 mmol, the time for complete reduction were 60 to 90, 180, and 390 min (Figure 1). We chose the ratio 1/200, that is 10 mmol of nitro compound was reduced over 0.05 mmol of BER-Pd.

Hydrogenation of Representative Aromatic Nitro Compounds over BER-Pd. Hydrogenation was carried out, using Brown automatic hydrogenator[4] at room temperature, 10 mmol of nitro compounds being hydrogenated over 0.05 mmol of Pd in BER-Pd. The results are summarized in Table 1.

As shown in Table 1, aromatic nitro compounds can be reduced to the corresponding amines in 1-6 h at room temperature in high yields without affecting ketone, ester, ether, hydroxy or nitrile groups also present. However, in the case of 4-chloronitrobenzene, we could obtain only 64% yield of chloroaniline together with 30% aniline, the dechlorinated